JOURNAL OF AIRCRAFT
Vol. 41, No. 2, March–April 2004

Mode Acceleration Based Random Gust Stresses in Aeroservoelastic Optimization

Frode Engelsen*
The Boeing Company, Seattle, Washington 98124
and
Eli Livne†
University of Washington, Seattle, Washington 98195-2400

The present paper describes a method for obtaining accurate design-oriented stress and stress-sensitivity information from reduced-order linear-time-invariant state-space models of integrated aeroservoelastic systems, using Lyapunov's Equation for calculating covariance matrices of the displacement and stress responses. A complete formulation of the reduced-order stress gust response problem for aeroservoelastic design synthesis, tailored toward integration with control-system design techniques based on modern control, is presented. It includes an adaptation of the mode-acceleration method, reduced-order analytic sensitivities of stress covariances, and efficient approximations to be used in a nonlinear programming/approximation concepts approach to design optimization. A realistic aeroservoelastic model of a typical passenger airplane is used as a test case, and the paper includes results of convergence studies for the assessment of order-reduction effects on the accuracy of the integrated structure/aerodynamic/control models.

Nomenclature

$[A]$, $[B]$, $[C]$, $[D]$	=	state-space model matrices (with appropriate subscripts to designate sensors, actuators, control laws, gust filter, and overall system)
$[A_{i\phi}]$	=	Roger aerodynamic matrices (real) for fitting $[A(s)][\phi]$ [Eq. (8)] $n_u \times n_q$
$[A(s)]$	=	Laplace transformed full-order influence coefficient matrix (associated with full-order structural model) $n_u \times n_u$
$[C]$	=	viscous damping matrix (structural)
c_i^s, c_i^g	=	aerodynamic lag terms for structural and gust forces, respectively
$[D]$	=	aerodynamic matrix in a minimum-state rational approximation form [Eq. (9)]
$[E]$	=	aerodynamic matrix in a minimum-state rational approximation form [Eq. (9)]
$[I]$	=	identity matrix
$[K]$	=	stiffness matrix
$[M]$	=	mass matrix
N_{Ls}	=	number of aerodynamic lag terms
n_A	=	order of the state-space model of the actuators
n_{CO}	=	order of state-space model of the multi-input/multi-output control law block
n_c	=	number of active control surfaces
n_g	=	order of the state-space model of the gust filter
n_{Lg}	=	number of lag terms in a minimum-state unsteady aerodynamic gust force rational approximation
n_{Ls}	=	number of lag terms in a minimum-state unsteady aerodynamic force rational approximation (structural and control-surface motions)
n_q	=	number of reduced-order structural degrees of freedom
n_u	=	full-order number of structural degrees of freedom
$[Q]$	=	intensity matrix of the white noise driving the gust filter
$\{\boldsymbol{q}\}$	=	vector of reduced-order generalized coordinates
q_D	=	dynamic pressure
$[S]$	=	matrix used to calculate stresses from full-order displacements
S_{ref}	=	wing reference area
s	=	Laplace variable
$\{s_{xx} \;\; s_{yy} \;\; s_{xy}\}^T$	=	vector of local stresses in a plane-stress thin structural element
U_∞	=	flight speed
$\{\boldsymbol{u}\}$	=	full-order displacement vector
w	=	vertical speed of atmospheric gusts
$[X]$	=	covariance matrix for complete aeroservoelastic system with structural degrees of freedom reduced by mode displacement basis
$\{\boldsymbol{x}\}$	=	state vector for complete aeroservoelastic system
$\{\boldsymbol{x}_i\}$	=	state vector for subsystem i
$\{y_{\mathrm{meas}}\}$	=	true structural responses at the points of measurement
$\{\boldsymbol{\delta}\}$	=	vector of commands to the actuators
$[\phi]$	=	matrix containing (column by column) reduced-order modal basis $n_u \times n_q$
$[\Phi_0]$, $[\Phi_1]$, $[\Phi_2]$	=	matrices defining [Eq. (17)] the true responses on the structure at the points of response measurement

Subscripts and Superscripts

A	=	actuator
CO	=	control law

Received 30 July 2001; revision received 10 May 2003; accepted for publication 11 May 2003.

*Associate Technical Fellow, Loads and Dynamics; frode.engelsen@boeing.com.

†Professor, Department of Aeronautics and Astronautics; eli@aa.washington.edu. Associate Fellow AIAA.

c	=	control degrees of freedom
cc	=	control-control partition of system matrices
cs	=	control-structural coupling in system matrices
G	=	gust filter
g	=	gust
s	=	structural degrees of freedom
sc	=	structural-control coupling in system matrices
SE	=	sensor
sg	=	structural-gust partition of system matrices
ss	=	structural-structural partition of system matrices
T	=	transpose

Introduction

RANDOM stresses caused by flight in turbulence,[1–4] superimposed on stresses as a result of steady maneuvers, must be taken into account in any effort to synthesize a flexible flight vehicle with or without an active control system.[5–8] Because the mathematical models of integrated actively controlled flight vehicles are large, some form of model order reduction becomes necessary,[9–11] whether frequency domain[12] or time domain analysis techniques[6,7,13,14] are used. For the structural dynamic part of the model, various structural dynamic order-reduction techniques have been widely used over the years, including various mode displacement (MD), Ritz vectors, modified mode displacement (Fictitious mass), mode acceleration (MA), and combined direct-adjoint methods, to name a few.[15–26]

A number of problems arise when such order-reduction methods are used for design optimization. First, in order to provide gradient-based optimization algorithms the information they require, derivatives of response functions (constraints and objectives), must be calculated in addition to the analysis values of the response functions themselves. Additionally, it is well known[8–11,25,26] that it is not straightforward, with the widely used displacement-method based models of structural dynamics, to obtain accurate stress information from reduced-order models (based on finite element or any Rayleigh–Ritz discretization). With structural dynamic models reduced-order stress design sensitivities are even more challenging to obtain.[25,26] A significant effort over the last 20 years has been aimed at formulation, order reduction, sensitivity, and approximation techniques that would make it possible to include constraints on combined maneuver/gust response stresses in integrated aeroservoelastic optimization in a practical way. The work in this area is still evolving. The present paper describes a method for obtaining accurate design-oriented stress and stress sensitivity information from reduced order linear-time-invariant state-space models of integrated aeroservoelastic systems, using Lyapunov's equation for calculating covariance matrices of the displacement and stress responses. Lyapunov's equations[27] have been used in modern control to obtain covariance terms of the response to random inputs for many years. The utilization of Lyapunov's equation for calculating gust response of aeroservoelastic systems has already been explored in a number of studies.[5–7,13,28,29] The emphasis, however, in most of those studies was on displacement and displacement-rate responses (such as accelerations at points on the structure, motion of control surfaces, and rate of motion of control surfaces). Here we present a complete and detailed formulation of the stress gust response problem for aeroservoelastic design synthesis, tailored toward integration with control system design techniques based on modern control. It includes order reduction based on an adaptation of the MA method, reduced-order analytic sensitivity of stress covariances, and efficient approximations to be used in a nonlinear programming/approximation concepts[30,31] approach to design optimization. The paper includes results of thorough convergence studies for assessment of the effect of order reduction on accuracy.

Formulation

Aeroelasticity

The partitioned Laplace-transformed equations corresponding to structural degrees of freedom of the linearized dynamic aeroelastic equations of motion for an actively controlled deformable airplane, based on full-order structural dynamic degrees of freedom, are

$$\left(s^2\begin{bmatrix}M^{ss} & M^{sc}\end{bmatrix}+s\begin{bmatrix}C^{ss} & C^{sc}\end{bmatrix}+\begin{bmatrix}K^{ss} & K^{sc}\end{bmatrix}\right)\begin{Bmatrix}u_s(s)\\ q_c(s)\end{Bmatrix} - q_D S_{\text{ref}}\begin{bmatrix}A^{ss}(s) & A^{sc}(s)\end{bmatrix}\begin{Bmatrix}u_s(s)\\ q_c(s)\end{Bmatrix} = q_D S_{\text{ref}}\{A^{sg}(s)\}[w_g(s)/U_\infty] \tag{1}$$

These equations can represent a free-free airplane in flight (the stiffness matrix $[K^{ss}]$ in this case will include rigid-body motions and become singular) or a restrained vehicle, in which case the stiffness matrix is nonsingular. General formulations of the free-free problem will further partition the system matrices into those associated with rigid-body motion and those associated with elastic modes of vibration. However, to simplify the derivations in the following paragraphs it is assumed here that the stiffness matrix $[K^{ss}]$ is always nonsingular. This does not limit the generality of the formulation used here significantly because free-free conditions can be always simulated by connecting the vehicle "numerically" to the ground using springs (in a statically determinate manner) that are soft enough to separate rigid-body motions from elastic motions.

Note that the full-order aerodynamic matrices $[A^{ss}(s)\ \ A^{sc}(s)]$, $\{A^{sg}(s)\}$ are not usually available with large-scale finite element structural models. They are calculated, using an aerodynamic mesh, for a set of motion shapes in the form of some vibration modes, polynomial functions, or Ritz vectors. In the case of modeling airplane wings and control surfaces using the equivalent-plate approach,[32–36] it is possible to create full-order aerodynamic matrices corresponding to all polynomial Ritz functions used for the different wing and control surface zones.[34,37] This difference has a bearing on the method developed here. The derivation assumes the availability of full-order aerodynamic matrices, corresponding to the full-order set of structural degrees of freedom. Adaptation to the case of structural finite element models is straightforward and is presented briefly in Appendix A.

Stresses at any point in the thin-walled structure can be calculated from the deformations using

$$\begin{Bmatrix}s_{xx}\\ s_{yy}\\ s_{xy}\end{Bmatrix} = [S]^T\{u_s\} \tag{2}$$

where different matrices $[S]$ are used for different points on the structure. The displacements can be approximated by a linear combination of lower-order mode shapes:

$$\{u_s\} = [\phi]\{q_s\} \tag{3}$$

where each column of the transformation matrix represents a single mode shape.

The reduced-order equations of motion will be (after premultiplication by $[\phi]^T$)

$$[\varphi]^T\left(s^2[M^{ss}]+s[C^{ss}]+[K^{ss}]-q_D S_{\text{ref}}[A^{ss}(s)]\right)[\varphi]\{q_s(s)\} + [\varphi]^T\left(s^2[M^{sc}]+s[C^{sc}]+[K^{sc}]-q_D S_{\text{ref}}[A^{sc}(s)]\right)\{q_c(s)\} = q_D S_{\text{ref}}[\varphi]^T\{A^{sg}(s)\}[w_g(s)/U_\infty] \tag{4}$$

Approximate stresses based on such a MD reduced-order model can, therefore, be calculated from [Eqs. (2) and (3)]

$$\begin{Bmatrix}s_{xx}\\ s_{yy}\\ s_{xy}\end{Bmatrix} = [S]^T\{u_s\} = [S]^T[\phi]\{q_s\} \tag{5}$$

However, it is well known[15–17] that the accuracy of MD stresses is poor. Unless special attention is paid to the capability to capture local effects when vectors for the reduced-order basis are selected,[25] conventional lower-order natural vibration modes cannot capture local effects associated with concentrated loading, local stresses, or sensitivities of stresses with respect to structural design variables.

Because improved stress and stress-sensitivity accuracy is obtained if the displacements used in Eq. (2) are calculated from a full-order structural model, the MA method is based on rewriting the full order Eq. (1) as

$$[K^{ss}]\{u_s(s)\} = \{F_s(s)\} \tag{6}$$

where the force vector on the right-hand side is obtained using approximate accelerations and velocities [Eq. (3)] obtained from the MD solution of Eq. (4). Thus,

$$\begin{aligned}\{F_s(s)\} &= -\big(s^2[M^{ss}] + s[C^{ss}] - q_D S_{\text{ref}}[A^{ss}(s)]\big)[\varphi]\{q_s(s)\} \\ &\quad - \big(s^2[M^{sc}] + s[C^{sc}] + [K^{sc}] - q_D S_{\text{ref}}[A^{sc}(s)]\big)\{q_c(s)\} \\ &\quad + q_D S_{\text{ref}}\{A^{sg}(s)\}[w_g(s)/U_\infty]\end{aligned} \tag{7}$$

The unsteady aerodynamic forces for the full-order equations (when the equivalent plate method is used), calculated for simple harmonic motion at discrete reduced frequencies, can be approximated by a rational function approximation as defined by Roger.[38] Because the fitted matrices are used in both the load equations (7) and in the MD equations of motion (4), the Roger fit is performed on the aerodynamics for the load equations. This means that only the columns of the structural degrees of freedom have been reduced to modal coordinates, but the rows remain full order (see Appendix A for the case of a finite element model). That is, a rational function approximation is first created for the frequency-dependent aerodynamic matrices $[A^{ss}(s)][\phi]$, $[A^{sc}(s)]$, and $[A^{sg}(s)]$.

$$\begin{aligned}[A^{ss}(s)][\varphi] &= \left[A^{ss}_{0\varphi}\right] + \left[A^{ss}_{1\varphi}\right]s + \left[A^{ss}_{2\varphi}\right]s^2 + \sum_{i=1}^{N_{Ls}} \frac{s}{s + c_i^s}\left[A^{ss}_{(i+2)\varphi}\right] \\ [A^{sc}(s)] &= \left[A^{sc}_0\right] + \left[A^{sc}_1\right]s + \left[A^{sc}_2\right]s^2 + \sum_{i=1}^{N_{Ls}} \frac{s}{s + c_i^s}\left[A^{sc}_{i+2}\right] \\ \{A^{sg}(s)\} &= \left\{A^g_0\right\} + \left\{A^g_1\right\}s + \sum_{i=1}^{N_{Lg}} \frac{s}{s + c_i^g}\left\{A^g_{i+2}\right\}\end{aligned} \tag{8}$$

It is assumed that the forces associated with structural and control degrees of freedom have the same aerodynamic lag poles c_i^s, but that the lags associated with gust c_i^g might be different. The generalized aerodynamic matrices to be used in the MD equations of motion [Eq. (4)] are obtained from the Roger matrices of Eq. (8) by premultiplying those matrices by $[\phi]^T$.

Alternatively, a minimum-state rational function approximation (MS) can be used to fit the frequency dependent aerodynamic matrices[39]:

$$\begin{aligned}[A^{ss}(s)\varphi \quad A^{sc}(s)] &= \left\lfloor A^{ss}_{0\varphi} \quad A^{sc}_0 \right\rfloor + \left\lfloor A^{ss}_{1\varphi} \quad A^{sc}_1 \right\rfloor s \\ &\quad + \left[A^{ss}_{2\varphi} \quad A^{sc}_2\right]s^2 + s\left[D^s_\varphi\right](s[I] - [R^s])^{-1}[E^s \quad E^c] \\ \{A^{sg}(s)\} &= \left\{A^g_0\right\} + \left\{A^g_1\right\}s + s[D^g](s[I] - [R^g])^{-1}\{E_g\}\end{aligned} \tag{9}$$

The matrices $[A_{i\phi}]$ and $[D_\phi]$ are then premultiplied by $[\phi]^T$ for use in the MD equations of motion [Eq. (4)]. The form of the MS fit [Eq. (9)] can also accommodate the Roger fit [Eq. (8)] and is used in the following developments.

Aerodynamic lag states are now introduced:

$$\begin{aligned}\{r_s(s)\} &= (s[I] - [R^s])^{-1}[E^s \quad E^c]s\begin{Bmatrix} q_s(s) \\ q_c(s)\end{Bmatrix} \\ \{r_g(s)\} &= (s[I] - [R^g])^{-1}\{E^g\}s w_g(s)\end{aligned} \tag{10}$$

leading to

$$\begin{aligned}s\{r_s\} &= [R^s]\{r_s\} + [E^s]s\{q_s(s)\} + [E^c]s\{q_c(s)\} \\ s\{r_g\} &= [R^g]\{r_g\} + \{E^g\}s w_g(s)\end{aligned} \tag{11}$$

These rational function expressions can now be inserted into the load equations [Eq. (7)]

$$\begin{aligned}\{F_s(s)\} &= \left[K^{ss}_\varphi\right]\{q_s(s)\} - \left(s^2\left\lfloor \hat{M}^{ss}_\varphi \right\rfloor + s\left\lfloor \hat{C}^{ss}_\phi \right\rfloor + \left\lfloor \hat{K}^{ss}_\varphi \right\rfloor\right)\{q_s(s)\} \\ &\quad - (s^2[\hat{M}^{sc}] + s[\hat{C}^{sc}] + [\hat{K}^{sc}])\{q_c(s)\} + q_D S_{\text{ref}}\left[D^s_\varphi\right]\{r_s(s)\} \\ &\quad + (q_D S_{\text{ref}}/U_\infty)[D^g]\{r_g(s)\} + (q_D S_{\text{ref}}/U_\infty)\left(\left\{A^g_0\right\}\right. \\ &\quad \left. + \left\{A^g_1\right\}s\right)w_g(s)\end{aligned} \tag{12}$$

where

$$\begin{aligned}\left[K^{ss}_\phi\right] &= [K^{ss}][\phi], \qquad \left[\hat{M}^{ss}_\phi\right] = [M^{ss}][\phi] - q_D S_{\text{ref}}\left[A^{ss}_{2\phi}\right] \\ \left[\hat{C}^{ss}_\phi\right] &= [C^{ss}][\phi] - q_D S_{\text{ref}}\left[A^{ss}_{1\phi}\right] \\ \left[\hat{K}^{ss}_\phi\right] &= [K^{ss}][\phi] - q_D S_{\text{ref}}\left[A^{ss}_{0\phi}\right]\end{aligned} \tag{13}$$

and

$$\begin{aligned}\lfloor \hat{M}^{sc} \rfloor &= [M^{sc}] - q_D S_{\text{ref}}\left[A^{sc}_2\right], \qquad [\hat{C}^{sc}] = [C^{sc}] - q_D S_{\text{ref}}\left[A^{sc}_1\right] \\ [\hat{K}^{sc}] &= [K^{sc}] - q_D S_{\text{ref}}\left[A^{sc}_0\right]\end{aligned} \tag{14}$$

The vector of generalized displacements $\{\boldsymbol{q}_s(s)\}$ on the right-hand side of Eq. (12) is the mode displacement solution. The aeroservoelastic MA method approximates the full-order load distribution by combining the full-order external forces with approximate inertial and damping forces (both structural and aerodynamic) obtained from the reduced-order MD solution. The coupling control surface/structure stiffness and damping matrices (corresponding to rigid control surface rotation caused by actuator commands) are zero by definition, that is, $[K^{sc}] = [0]$ and $[C^{sc}] = [0]$. A possible definition of the full-order viscous damping matrix in the structural dynamic equations is discussed in Appendix B.

The MD equations of motion [Eq. (4)] can now be written as

$$\begin{aligned}&\left(s^2[\varphi]^T\left\lfloor \hat{M}^{ss}_\varphi \right\rfloor + s[\varphi]^T\left\lfloor \hat{C}^{ss}_\varphi \right\rfloor + [\varphi]^T\left\lfloor \hat{K}^{ss}_\varphi \right\rfloor\right)\{q_s(s)\} \\ &\quad + \left(s^2[\varphi]^T[\hat{M}^{sc}] + s[\varphi]^T[\hat{C}^{sc}] + [\varphi]^T[\hat{K}^{sc}]\right)\{q_c(s)\} \\ &\quad - q_D S_{\text{ref}}[\varphi]^T\left[D^s_\varphi\right]\{r_s(s)\} - (q_D S_{\text{ref}}/U_\infty)[\varphi]^T[D^g]\{r_g(s)\} \\ &\quad = (q_D S_{\text{ref}}/U_\infty)\left([\varphi]^T\{A^g_0\} + [\varphi]^T\{A^g_1\}s\right)w_g(s)\end{aligned} \tag{15}$$

To obtain a desired frequency content of the gust excitation velocity, it is modeled as the output of a linear filter subjected to white noise input $\{w(s)\}$.

$$s\{x_g(s)\} = [A_g]\{x_g(s)\} + \{B_g\}w(s), \qquad w_g(s) = \lfloor C_g \rfloor\{x_g(s)\} \tag{16}$$

Measurement, Actuation, and Control

The measured responses on the structure can be displacements, velocities, or accelerations. Using Eq. (3), the "true" responses at the points where they are measured can be obtained from

$$\begin{aligned}\{y_{\text{meas}}(s)\} &= \left([\Phi_0] + [\Phi_1]s + [\Phi_2]s^2\right)\{u_s(s)\} \\ &= \left([\Phi_0][\phi] + [\Phi_1][\phi]s + [\Phi_2][\phi]s^2\right)\{q_s(s)\}\end{aligned} \tag{17}$$

Note that the matrices $[\Phi_i]$ determine contribution of different degrees of freedom to the actual response, whereas the matrix $[\phi]$ is the matrix containing mode shape vectors.

The measurement signals available to the control system are the outputs of sensors modeled by

$$s\{x_{\mathrm{SE}}(s)\} = [A_{\mathrm{SE}}]\{x_{\mathrm{SE}}(s)\} + [B_{\mathrm{SE}}]\{y_{\mathrm{meas}}(s)\}$$

$$\{y_{\mathrm{SE}}(s)\} = [C_{\mathrm{SE}}]\{x_{\mathrm{SE}}(s)\} \tag{18}$$

The actuator dynamics, from actuator command to control-surface rotation, assuming irreversible controls, are

$$s\{x_A(s)\} = [A_A]\{x_A(s)\} + [B_A]\{\delta(s)\}$$

$$\{q_c(s)\} = [C_A]\{x_A(s)\} \tag{19}$$

The control law (actuator commands caused by sensor measurements) is

$$s\{x_{\mathrm{CO}}(s)\} = [A_{\mathrm{CO}}]\{x_{\mathrm{CO}}(s)\} + [B_{\mathrm{CO}}]\{y_{\mathrm{SE}}(s)\}$$

$$\{\delta(s)\} = [C_{\mathrm{CO}}]\{x_{\mathrm{CO}}(s)\} + [D_{\mathrm{CO}}]\{y_{\mathrm{SE}}(s)\} \tag{20}$$

Note that the state-space models for the gust filter, sensors, and actuators are all strictly proper. The control law model allows proper transfer functions, that is, in the control block of equations [Eq. (20)] the D matrix can be nonzero.

The vector of control surface motions $\{\boldsymbol{q}_c\}$ is available from Eq. (19). Examination of Eqs. (12) and (15) shows that expressions for the rates sw_g, $s\{q_c\}$, and $s^2\{q_c\}$ are also required. When the time derivative of the output in Eq. (16) is taken,

$$\begin{Bmatrix} w_g(s) \\ sw_g(s) \end{Bmatrix} = \begin{bmatrix} C_g \\ C_g A_g \end{bmatrix} \{x_g(s)\} + \begin{Bmatrix} 0 \\ C_g B_g \end{Bmatrix} w(s) \tag{21}$$

From Eqs. (17) and (18),

$$\begin{Bmatrix} y_{\mathrm{SE}}(s) \\ sy_{\mathrm{SE}}(s) \end{Bmatrix} = \begin{bmatrix} C_{\mathrm{SE}} \\ C_{\mathrm{SE}} A_{\mathrm{SE}} \end{bmatrix} \{x_{\mathrm{SE}}(s)\}$$

$$+ \begin{bmatrix} 0 \\ C_{\mathrm{SE}} B_{\mathrm{SE}} \end{bmatrix} \left([\Phi_0\phi] + [\Phi_1\phi]s + [\Phi_2\phi]s^2\right)\{q_s(s)\} \tag{22}$$

With the derivative of the output in Eq. (19), we get.

$$\begin{Bmatrix} q_c(s) \\ sq_c(s) \\ s^2 q_c(s) \end{Bmatrix} = \begin{bmatrix} C_A \\ C_A A_A \\ C_A A_A A_A \end{bmatrix} \{x_A(s)\}$$

$$+ \begin{bmatrix} 0 & 0 \\ C_A B_A & 0 \\ C_A A_A B_A & C_A B_A \end{bmatrix} \begin{Bmatrix} \delta(s) \\ s\delta(s) \end{Bmatrix} \tag{23}$$

And from Eq. (20) for the output of the control law equations,

$$\begin{Bmatrix} \delta(s) \\ s\delta(s) \end{Bmatrix} = \begin{bmatrix} C_{\mathrm{CO}} \\ C_{\mathrm{CO}} A_{\mathrm{CO}} \end{bmatrix} \{x_{\mathrm{CO}}(s)\} + \begin{bmatrix} D_{\mathrm{CO}} & 0 \\ C_{\mathrm{CO}} B_{\mathrm{CO}} & D_{\mathrm{CO}} \end{bmatrix} \begin{Bmatrix} y_{\mathrm{SE}}(s) \\ sy_{\mathrm{SE}}(s) \end{Bmatrix} \tag{24}$$

Combining Eqs. (23) and (24),

$$\begin{Bmatrix} q_c(s) \\ sq_c(s) \\ s^2 q_c(s) \end{Bmatrix} = \begin{bmatrix} C_A \\ C_A A_A \\ C_A A_A A_A \end{bmatrix} \{x_A(s)\}$$

$$+ \begin{bmatrix} 0 \\ C_A B_A C_{\mathrm{CO}} \\ C_A A_A B_A C_{\mathrm{CO}} + C_A B_A C_{\mathrm{CO}} A_{\mathrm{CO}} \end{bmatrix} \{x_{\mathrm{CO}}(s)\}$$

$$+ \begin{bmatrix} 0 & 0 \\ C_A B_A D_{\mathrm{CO}} & 0 \\ C_A A_A B_A D_{\mathrm{CO}} + C_A B_A C_{\mathrm{CO}} B_{\mathrm{CO}} & C_A B_A D_{\mathrm{CO}} \end{bmatrix} \begin{Bmatrix} y_{\mathrm{SE}}(s) \\ sy_{\mathrm{SE}}(s) \end{Bmatrix} \tag{25}$$

When Eq. (22) is now used, we get

$$\begin{Bmatrix} q_c(s) \\ sq_c(s) \\ s^2 q_c(s) \end{Bmatrix} = \begin{bmatrix} C_A \\ C_A A_A \\ C_A A_A A_A \end{bmatrix} \{x_A(s)\}$$

$$+ \begin{bmatrix} 0 \\ C_A B_A C_{\mathrm{CO}} \\ C_A A_A B_A C_{\mathrm{CO}} + C_A B_A C_{\mathrm{CO}} A_{\mathrm{CO}} \end{bmatrix} \{x_{\mathrm{CO}}(s)\}$$

$$+ \begin{bmatrix} 0 \\ C_A B_A D_{\mathrm{CO}} C_{\mathrm{SE}} \\ C_A A_A B_A D_{\mathrm{CO}} C_{\mathrm{SE}} + C_A B_A C_{\mathrm{CO}} B_{\mathrm{CO}} C_{\mathrm{SE}} + C_A B_A D_{\mathrm{CO}} C_{\mathrm{SE}} A_{\mathrm{SE}} \end{bmatrix}$$

$$\times \{x_{\mathrm{SE}}(s)\} + \begin{bmatrix} 0 \\ 0 \\ C_A B_A D_{\mathrm{CO}} C_{\mathrm{SE}} B_{\mathrm{SE}} \end{bmatrix}$$

$$\times \left([\Phi_0\phi] + [\Phi_1\phi]s + [\Phi_2\phi]s^2\right)\{q_s(s)\} \tag{26}$$

Equations (21) and (26) can now be used in the load equation, Eq. (12).

$$\begin{aligned}
\{F_s(s)\} = &-\left\lfloor \hat{M}^{ss}_{\varphi} + \hat{M}^{sc} C_A B_A D_{\mathrm{CO}} C_{\mathrm{SE}} B_{\mathrm{SE}} \Phi_2 \varphi \right\rfloor s^2 \{q_s(s)\} \\
&+ \left(\left[K^{ss}_{\phi}\right] - \left[\hat{K}^{ss}_{\phi} + \hat{M}^{sc} C_A B_A D_{\mathrm{CO}} C_{\mathrm{SE}} B_{\mathrm{SE}} \Phi_0 \varphi\right]\right)\{q_s(s)\} \\
&- \left[\hat{C}^{ss}_{\phi} + \hat{M}^{sc} C_A B_A D_{\mathrm{CO}} C_{\mathrm{SE}} B_{\mathrm{SE}} \Phi_1 \varphi\right] s\{q_s(s)\} \\
&- \left(\left[\hat{K}^{sc} C_A\right] + \left[\hat{C}^{sc} C_A A_A\right] + \left[\hat{M}^{sc} C_A A_A A_A\right]\right)\{x_A(s)\} \\
&- \left(\left[\hat{C}^{sc} C_A B_A D_{\mathrm{CO}} C_{\mathrm{SE}}\right] + \left[\hat{M}^{sc} C_A A_A B_A D_{\mathrm{CO}} C_{\mathrm{SE}}\right]\right. \\
&\left. + \left[\hat{M}^{sc} C_A B_A C_{\mathrm{CO}} B_{\mathrm{CO}} C_{\mathrm{SE}}\right] + \left[\hat{M}^{sc} C_A B_A D_{\mathrm{CO}} C_{\mathrm{SE}} A_{\mathrm{SE}}\right]\right) \\
&\times \{x_{\mathrm{SE}}(s)\} - \left(\left[\hat{C}^{sc} C_A B_A C_{\mathrm{CO}}\right] + \left[\hat{M}^{sc} C_A A_A B_A C_{\mathrm{CO}}\right]\right. \\
&\left. + \left[\hat{M}^{sc} C_A B_A C_{\mathrm{CO}} A_{\mathrm{CO}}\right]\right)\{x_{\mathrm{CO}}(s)\} + (q_D S_{\mathrm{ref}}/U_{\infty})\left(\left[A^g_0 C_g\right]\right. \\
&\left. + \left[A^g_1 C_g A_g\right]\right)\{x_g(s)\} + q_D S_{\mathrm{ref}}\left[D^s_{\phi}\right]\{r_s\} \\
&+ (q_D S_{\mathrm{ref}}/U_{\infty})[D^g]\{r_g\} + (q_D S_{\mathrm{ref}}/U_{\infty})\left\{A^g_1 C_g B_g\right\} w(s)
\end{aligned} \tag{27}$$

Equations (21) and (26) can also be substituted into the MD equations of motion, Eq. (15), to yield

$$\begin{aligned}
[\varphi]^T &\left\lfloor \hat{M}^{ss}_{\varphi} + \hat{M}^{sc} C_A B_A D_{\mathrm{CO}} C_{\mathrm{SE}} B_{\mathrm{SE}} \Phi_2 \varphi \right\rfloor s^2 \{q_s(s)\} \\
&= -[\varphi]^T \left[\hat{K}^{ss}_{\varphi} + \hat{M}^{sc} C_A B_A D_{\mathrm{CO}} C_{\mathrm{SE}} B_{\mathrm{SE}} \Phi_0 \varphi\right]\{q_s(s)\} \\
&- [\varphi]^T \left[\hat{C}^{ss}_{\varphi} + \hat{M}^{sc} C_A B_A D_{\mathrm{CO}} C_{\mathrm{SE}} B_{\mathrm{SE}} \Phi_1 \varphi\right] s\{q_s(s)\} \\
&- [\varphi]^T \left(\left[\hat{K}^{sc} C_A\right] + \left[\hat{C}^{sc} C_A A_A\right] + \left[\hat{M}^{sc} C_A A_A A_A\right]\right)\{x_A(s)\} \\
&- [\varphi]^T \left(\left[\hat{C}^{sc} C_A B_A D_{\mathrm{CO}} C_{\mathrm{SE}}\right] + \left[\hat{M}^{sc} C_A A_A B_A D_{\mathrm{CO}} C_{\mathrm{SE}}\right]\right. \\
&\left. + \left[\hat{M}^{sc} C_A B_A C_{\mathrm{CO}} B_{\mathrm{CO}} C_{\mathrm{SE}}\right] + \left[\hat{M}^{sc} C_A B_A D_{\mathrm{CO}} C_{\mathrm{SE}} A_{\mathrm{SE}}\right]\right) \\
&\times \{x_{\mathrm{SE}}(s)\} - [\varphi]^T \left(\left[\hat{C}^{sc} C_A B_A C_{\mathrm{CO}}\right] + \left[\hat{M}^{sc} C_A A_A B_A C_{\mathrm{CO}}\right]\right. \\
&\left. + \left[\hat{M}^{sc} C_A B_A C_{\mathrm{CO}} A_{\mathrm{CO}}\right]\right)\{x_{\mathrm{CO}}(s)\} + (q_D S_{\mathrm{ref}}/U_{\infty})[\varphi]^T \left(\left[A^g_0 C_g\right]\right. \\
&\left. + \left[A^g_1 C_g A_g\right]\right)\{x_g(s)\} + q_D S_{\mathrm{ref}}[\varphi]^T \left[D^s_{\varphi}\right]\{r_s\} \\
&+ (q_D S_{\mathrm{ref}}/U_{\infty})[\varphi]^T [D^g]\{r_g\} \\
&+ (q_D S_{\mathrm{ref}}/U_{\infty})[\varphi]^T \left\{A^g_1 C_g B_g\right\} w(s)
\end{aligned} \tag{28}$$

In the following steps the output equations [of Eqs. (18) and (20)] are inserted into the state-space equation (19). This leads to

$$s\{x_A(s)\} = [A_A]\{x_A(s)\}+[B_A C_{CO}]\{x_{CO}(s)\}+[B_A D_{CO} C_{SE}]\{x_{SE}(s)\} \tag{29}$$

Equation (17) is inserted into the state-space equation (18):

$$-[B_{SE}\Phi_2\phi]s^2\{q_s(s)\} + s\{x_{SE}(s)\} = [B_{SE}\Phi_0\phi]\{q_s(s)\} + [B_{SE}\Phi_1\phi]s\{q_s(s)\} + [A_{SE}]\{x_{SE}(s)\} \tag{30}$$

Equations (18) and (20) are now used to obtain

$$s\{x_{CO}(s)\} = [A_{CO}]\{x_{CO}(s)\} + [B_{CO}C_{SE}]\{x_{SE}(s)\} \tag{31}$$

And the gust filter Eq. (16)

$$s\{x_g(s)\} = [A_g]\{x_g(s)\} + \{B_g\}w(s) \tag{32}$$

Finally the state-space equations for the aerodynamic states are obtained from Eqs. (11) and (26):

$$s\{r_s\} = [E^s]s\{q_s(s)\} + \left[E^c C_A A_A\right]\{x_A(s)\} + \left[E^c C_A B_A D_{CO} C_{SE}\right] \times \{x_{SE}(s)\} + \left[E^c C_A B_A C_{CO}\right]\{x_{CO}(s)\} + [R^s]\{r_s\} \tag{33}$$

and the equations for the added gust aerodynamic states are obtained from Eqs. (11) and (21):

$$s\{r_g\} = \left[E^g C_g A_g\right]\{x_g(s)\} + [R^g]\{r_g\} + \left\{E^g C_g B_g\right\}w(s) \tag{34}$$

Complete Aeroservoelastic System

The state-space equations for the complete closed-loop system can now be assembled, after defining the system's state-space vector:

$$\{x\}^T = \left\lfloor \{x_1\}^T \quad \{x_2\}^T \quad \{x_A\}^T \quad \{x_{SE}\}^T \quad \{x_{CO}\}^T \quad \{x_g\}^T \quad \{r_s\}^T \quad \{r_g\}^T \right\rfloor \tag{35a}$$

where

$$\begin{matrix}\{x_1\} = \{q_s\} \\ \{x_2\} = s\{q_s\}\end{matrix} \quad \Rightarrow \quad s\{x_1\} = \{x_2\} \tag{35b}$$

In an effort to adopt a more concise notation, the load equation can now be written in the form:

$$\{F_s(s)\} = -[\bar{U}_{22}]s\{x_2(s)\} + \left(\left[K_\phi^{ss}\right] + [\bar{V}_{21}]\right)\{x_1(s)\} + [\bar{V}_{22}]\{x_2(s)\} + [\bar{V}_{23}]\{x_A(s)\} + [\bar{V}_{24}]\{x_{SE}(s)\} + [\bar{V}_{25}]\{x_{CO}(s)\} + [\bar{V}_{26}]\{x_g(s)\} + [\bar{V}_{27}]\{r_s\} + [\bar{V}_{28}]\{r_g\} + \{\bar{W}_2\}w(s) \tag{36}$$

where

$$[\bar{U}_{22}] = \left\lfloor \hat{M}_\phi^{ss} + \hat{M}^{sc} C_A B_A D_{CO} C_{SE} B_{SE}\Phi_2\phi \right\rfloor$$

$$[\bar{V}_{21}] = -\left[\hat{K}_\phi^{ss} + \hat{M}^{sc} C_A B_A D_{CO} C_{SE} B_{SE}\Phi_0\phi\right]$$

$$[\bar{V}_{22}] = -\left[\hat{C}_\phi^{ss} + \hat{M}^{sc} C_A B_A D_{CO} C_{SE} B_{SE}\Phi_1\phi\right]$$

$$[\bar{V}_{23}] = -\left(\left\lfloor \hat{K}^{sc} C_A \right\rfloor + \left\lfloor \hat{C}^{sc} C_A A_A \right\rfloor + \left\lfloor \hat{M}^{sc} C_A A_A A_A \right\rfloor\right)$$

$$[\bar{V}_{24}] = -\left(\left[\hat{C}^{sc} C_A B_A D_{CO} C_{SE}\right] + \left[\hat{M}^{sc} C_A A_A B_A D_{CO} C_{SE}\right] + \left[\hat{M}^{sc} C_A B_A C_{CO} B_{CO} C_{SE}\right] + \left[\hat{M}^{sc} C_A B_A D_{CO} C_{SE} A_{SE}\right]\right)$$

$$[\bar{V}_{25}] = -\left(\left[\hat{C}^{sc} C_A B_A C_{CO}\right] + \left[\hat{M}^{sc} C_A A_A B_A C_{CO}\right] + \left[\hat{M}^{sc} C_A B_A C_{CO} A_{CO}\right]\right)$$

$$[\bar{V}_{26}] = (q_D S_{ref}/U_\infty)\left(\left[A_0^g C_g\right] + \left[A_1^g C_g A_g\right]\right)$$

$$[\bar{V}_{27}] = q_D S_{ref}\left[D_\phi^s\right], \qquad [\bar{V}_{28}] = (q_D S_{ref}/U_\infty)[D^g]$$

$$\{\bar{W}_2\} = (q_D S_{ref}/U_\infty)\left\{A_1^g C_g B_g\right\} \tag{37}$$

Equation (36) can be written in a more compact form as

$$\{F_s(s)\} = -[\bar{U}_{22}]s\{x_2(s)\} + [\bar{V}_2]\{x(s)\} + \{\bar{W}_2\}w(s) \tag{38}$$

where

$$[\bar{V}_2] = \left[K_\phi^{ss} + \bar{V}_{21} \quad \bar{V}_{22} \quad \bar{V}_{23} \quad \bar{V}_{24} \quad \bar{V}_{25} \quad \bar{V}_{26} \quad \bar{V}_{27} \quad \bar{V}_{28}\right] \tag{39}$$

Now, the MD aeroservoelastic equations of motion, Eq. (28), can be written in a similar form:

$$[U_{22}]s\{x_2(s)\} = [V_{21}]\{x_1(s)\} + [V_{22}]\{x_2(s)\} + [V_{23}]\{x_A(s)\} + [V_{24}]\{x_{SE}(s)\} + [V_{25}]\{x_{CO}(s)\} + [V_{26}]\{x_g(s)\} + [V_{27}]\{r_s\} + [V_{28}]\{r_g\} + \{W_2\}w(s) \tag{40}$$

where the equation of motion corresponding to structural degrees of freedom is reduced in order by premultiplication by $[\phi]^T$. Define

$$[U_{22}] = [\phi]^T\lfloor\bar{U}_{22}\rfloor$$

$$[V_{2j}] = [\phi]^T[\bar{V}_{2j}] \qquad j = 1, \ldots, 8$$

$$\{W_2\} = [\phi]^T\{\bar{W}_2\} \tag{41}$$

and the preceding equations (29–34) can be collected to create coupled aeroservoelastic equations of motion in the form:

$$s[U]\{x(s)\} = [V]\{x(s)\} + \{W\}w(s) \tag{42}$$

Examination of the matrices $[U]$ and $[V]$ reveals that they are of the form:

$$[U] = \begin{bmatrix} I & 0 & 0 & 0 & 0 & 0 & 0 & 0 \\ 0 & U_{22} & 0 & 0 & 0 & 0 & 0 & 0 \\ 0 & 0 & I & 0 & 0 & 0 & 0 & 0 \\ 0 & U_{42} & 0 & I & 0 & 0 & 0 & 0 \\ 0 & 0 & 0 & 0 & I & 0 & 0 & 0 \\ 0 & 0 & 0 & 0 & 0 & I & 0 & 0 \\ 0 & 0 & 0 & 0 & 0 & 0 & I & 0 \\ 0 & 0 & 0 & 0 & 0 & 0 & 0 & I \end{bmatrix} \tag{43}$$

$$[V] = \begin{bmatrix} 0 & I & 0 & 0 & 0 & 0 & 0 & 0 \\ V_{21} & V_{22} & V_{23} & V_{24} & V_{25} & V_{26} & V_{27} & V_{28} \\ 0 & 0 & V_{33} & V_{34} & V_{35} & 0 & 0 & 0 \\ V_{41} & V_{42} & 0 & V_{44} & 0 & 0 & 0 & 0 \\ 0 & 0 & 0 & V_{54} & V_{55} & 0 & 0 & 0 \\ 0 & 0 & 0 & 0 & 0 & V_{66} & 0 & 0 \\ 0 & V_{72} & V_{73} & V_{74} & V_{75} & 0 & V_{77} & 0 \\ 0 & 0 & 0 & 0 & 0 & V_{86} & 0 & V_{88} \end{bmatrix} \tag{44}$$

$$\{W\}^T = \left\lfloor 0 \quad W_2^T \quad 0 \quad 0 \quad 0 \quad W_6^T \quad 0 \quad W_8^T \right\rfloor \tag{45}$$

where

$$[V_{33}] = [A_A], \qquad [V_{34}] = [B_A D_{CO} C_{SE}], \qquad [V_{35}] = [B_A C_{CO}]$$

$$[U_{42}] = -[B_{SE}\Phi_2\phi], \qquad [V_{41}] = [B_{SE}\Phi_0\phi]$$

$$[V_{42}] = [B_{SE}\Phi_1\phi], \qquad [V_{44}] = [A_{SE}]$$

$$[V_{54}] = [B_{CO}C_{SE}], \qquad [V_{55}] = [A_{CO}]$$

$$[V_{66}] = \lfloor A_g \rfloor, \qquad \{W_6\} = \{B_g\}$$

$$[V_{72}] = [E^s], \qquad [V_{73}] = [E^c C_A A_A]$$

$$[V_{74}] = [E^c C_A B_A D_{CO} C_{SE}], \qquad [V_{75}] = [E^c C_A B_A C_{CO}]$$

$$[V_{77}] = [R^s]$$

$$[V_{86}] = \left[E^g C_g A_g\right], \qquad [V_{88}] = [R^g]$$

$$\{W_8\} = \left\{E^g C_g B_g\right\} \tag{46}$$

The state-space equations of motion can also be written as

$$s\{x(s)\} = [\tilde{A}]\{x(s)\} + \{\tilde{F}\}w(s) \tag{47}$$

where

$$[\tilde{A}] = [U]^{-1}[V], \qquad \{\tilde{F}\} = [U]^{-1}\{W\} \tag{48}$$

The second row partition of these equations [corresponding to Eq. (40) and the partitions in Eqs. (43–46)] gives an expression for $s^2\{q_s\}$:

$$s^2\{q_s\} = s\{x_2\} = [U_{22}]^{-1}[V_2]\{x(s)\} + [U_{22}]^{-1}\{W_2\}w(s) \tag{49}$$

where

$$[V_2] = [V_{21} \quad V_{22} \quad V_{23} \quad V_{24} \quad V_{25} \quad V_{26} \quad V_{27} \quad V_{28}] \tag{50}$$

This means that the summation of forces for the right-hand side of Eq. (6) can be written in terms of the state-space vector [Eqs. (38) and (49)]:

$$\{F_s(s)\} = [A_L]\{x(s)\} + \{F_L\}w(s) \tag{51}$$

where

$$[A_L] = [\bar{V}_2] - [\bar{U}_{22}][U_{22}]^{-1}[V_2]$$

$$\{F_L\} = \{\bar{W}_2\} - [\bar{U}_{22}][U_{22}]^{-1}\{W_2\} \tag{52}$$

Stress Retrieval

Having found a solution to the coupled aeroservoelastic problem (with MD-order reduction for the structural degrees of freedom) Eq. (47), we can use Eq. (6) to retrieve stresses, using the full-order stiffness matrix. In a displacement-based finite element or Rayleigh–Ritz method, stresses at a point (on a plane stress element) can be calculated from

$$\begin{Bmatrix} s_{xx}(s) \\ s_{yy}(s) \\ s_{xy}(s) \end{Bmatrix} = [S]^T\{u_s(s)\} = [S]^T[K^{ss}]^{-1}\{F_s(s)\} \tag{53}$$

An adjoint matrix is defined as follows:

$$[\eta]^T = [S]^T[K^{ss}]^{-1} \tag{54}$$

Because of the symmetry of the stiffness matrix, this leads to

$$[K^{ss}][\eta] = [S] \tag{55}$$

The matrix $[S]$ is static and is different for every point at which stresses are calculated. A corresponding adjoint matrix $[\eta]$ at each stress recovery point can be found from Eq. (55). Dynamic stresses can now be calculated using

$$\begin{Bmatrix} s_{xx}(s) \\ s_{yy}(s) \\ s_{xy}(s) \end{Bmatrix} = [\eta]^T\{F_s(s)\} \tag{56}$$

where the stresses and the force vector are dynamic. The covariance matrix of the three stress components is

$$[\mathrm{Cov}_s] = E\left(\begin{Bmatrix} s_{xx} \\ s_{yy} \\ s_{xy} \end{Bmatrix}\begin{Bmatrix} s_{xx} \\ s_{yy} \\ s_{xy} \end{Bmatrix}^T\right)$$

$$= [\eta]^T E\left(\{F_s\}\{F_s\}^T\right)[\eta] = [\eta]^T[\Gamma][\eta] \tag{57}$$

Gust Filter—Modeling Considerations

Examination of the expressions for the load vector [Eqs. (38) and (51)] reveals a direct dependency on the white noise input. Thus, the covariance matrix of the full-order forces is only finite if $\{F_L\} = \{0\}$. Inspection of equations (37) and (52) reveals that this is the case

$$\{\bar{W}_2\} = (q_D S_{\mathrm{ref}}/U_\infty)\left\{A_1^g C_g B_g\right\} = \{0\} \tag{58}$$

Thus, we must require that either $\{A_1^g\} = \{0\}$ or $C_g B_g = 0$. In the rational function approximation of the gust vector, $\{A_1^g\} = \{0\}$ can be utilized without much loss in accuracy if one of the lag poles is large compared to the frequency range of interest. In this case $s/(s + c_i^g) \approx s/c_i^g$, that is, proportional to s, and the matrix corresponding to this lag term will model the effect of the unused $\{A_1^g\}$. Alternatively, the matrix product $C_g B_g = 0$ for the gust filter transfer function if the order of the denominator is greater than the order of its numerator by at least two. In most common approximations of gust filter transfer functions, there is only a first-order difference between the denominator and the numerator. This can be overcome by either adding a low-pass filter to the gust filter[13] or by converting the filter from the form:

$$\frac{w_g}{w} = \frac{c_{n-1}s^{n-1} + \cdots + c_1 s + c_0}{s^n + d_{n-1}s^{n-1} + \cdots + d_1 s + d_0} \tag{59}$$

to

$$\frac{w_g}{w} = \frac{c_{n-1}s^{n-1} + \cdots + c_1 s + c_0}{\varepsilon s^{n+1} + s^n + d_{n-1}s^{n-1} + \cdots + d_1 s + d_0} \tag{60}$$

by adding a $(n+1)$th-order term with a small positive coefficient ε. This introduces an additional gust filter state in the model with a real negative lag pole close to $-1/\varepsilon$.

Figure 1 shows a comparison between the exact von Kármán and the two third-order ($n = 3$) rational approximations determined by Eqs. (59) and (60) for a typical flight condition. The exact spectrum rolls off with a slope of $-\frac{5}{3}$, while the standard rational model[40] will have an integer slope of -2. The new rational model will be identical to the standard rational model up to a frequency of $1/\varepsilon$ and will then

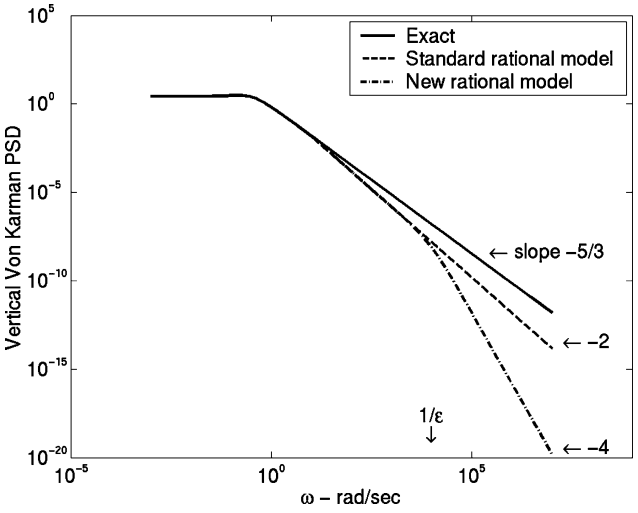

Fig. 1 Comparison of vertical spectra for the von Kármán and two rational approximations.

roll off with a slope of -4 above this frequency. The coefficient ε must therefore be chosen small enough such that $1/\varepsilon$ is higher than the highest frequency of interest. In the following example $\varepsilon = 0.0001$, which corresponds to a frequency of 1000 rad/s.

In the following it is assumed that

$$\{F_L\} = \{0\} \tag{61}$$

and Eq. (51) becomes

$$\{F_s(s)\} = [A_L]\{x(s)\} \tag{62}$$

Covariance Matrices of Full-Order Loads and Aeroservoelastic Mode-Displacement States

With Eq. (62) the covariance matrix of the full-order load elements become

$$[\Gamma] = E\left(\{F_s\}\{F_s\}^T\right) = [A_L]E(\{x\}\{x\}^T)[A_L]^T = [A_L][X][A_L]^T \tag{63}$$

where

$$[X] = E(\{x\}\{x\}^T) \tag{64}$$

is the covariance of the states-space degrees of freedom found from the Lyapunov's equation[27] for the MD reduced-order coupled aeroservoelastic system:

$$[\tilde{A}][X] + [X][\tilde{A}]^T = -\{\tilde{F}\}Q\{\tilde{F}\}^T \tag{65}$$

The intensity of the white noise input w is assumed to be Q.

$$E[w(t)w(\tau)^T] = Q\delta(t-\tau) \tag{66}$$

where $\delta(t)$ is the Dirac delta function.

Behavior Sensitivities

The sensitivity of gust stresses to changes in the design variables can be determined from the sensitivity of $[\mathrm{Cov}_s]$. Equation (57) is differentiated with respect to a design variable p:

$$\left[\frac{\partial \mathrm{Cov}_s}{\partial p}\right] = \left[\frac{\partial \eta}{\partial p}\right]^T [\Gamma][\eta] + [\eta]^T \left[\frac{\partial \Gamma}{\partial p}\right][\eta] + [\eta]^T[\Gamma]\left[\frac{\partial \eta}{\partial p}\right] \tag{67}$$

where

$$\left[\frac{\partial \Gamma}{\partial p}\right] = \left[\frac{\partial A_L}{\partial p}\right][X][A_L]^T + [A_L]\left[\frac{\partial X}{\partial p}\right][A_L]^T + [A_L][X]\left[\frac{\partial A_L}{\partial p}\right]^T \tag{68}$$

The sensitivity matrix $[\partial\eta/\partial p]$ can be determined by taking the derivative of Eq. (55) with respect to the design variable p.

$$[K^{ss}]\left[\frac{\partial \eta}{\partial p}\right] = -\left[\frac{\partial K^{ss}}{\partial p}\right][\eta] \tag{69}$$

Furthermore, from Eq. (52)

$$\left[\frac{\partial A_L}{\partial p}\right] = \left[\frac{\partial \bar{V}_2}{\partial p}\right] - \left[\frac{\partial \bar{U}_{22}}{\partial p}\right][U_{22}]^{-1}[V_2] - [\bar{U}_{22}]\frac{\partial [U_{22}]^{-1}}{\partial p}[V_2] - [\bar{U}_{22}][U_{22}]^{-1}\left[\frac{\partial V_2}{\partial p}\right] \tag{70}$$

We can differentiate $[U_{22}]^{-1}[U_{22}] = [I]$ to get

$$\frac{\partial [U_{22}]^{-1}}{\partial p} = -[U_{22}]^{-1}\frac{\partial [U_{22}]}{\partial p}[U_{22}]^{-1} \tag{71}$$

Then, from Eqs. (70) and (71):

$$\left[\frac{\partial A_L}{\partial p}\right] = \left[\frac{\partial \bar{V}_2}{\partial p}\right] - \left[\frac{\partial \bar{U}_{22}}{\partial p}\right][U_{22}]^{-1}[V_2] + [\bar{U}_{22}][U_{22}]^{-1} \times \frac{\partial [U_{22}]}{\partial p}[U_{22}]^{-1}[V_2] - [\bar{U}_{22}][U_{22}]^{-1}\left[\frac{\partial V_2}{\partial p}\right] \tag{72}$$

The sensitivity of the aeroservoelastic modally reduced state covariance matrix $[\partial X/\partial p]$ can be determined by differentiating Eq. (65) with respect to p:

$$[\tilde{A}]\left[\frac{\partial X}{\partial p}\right] + \left[\frac{\partial X}{\partial p}\right][\tilde{A}]^T = -\left\{\frac{\partial \tilde{F}}{\partial p}\right\}Q\{\tilde{F}\}^T - \{\tilde{F}\}Q\left\{\frac{\partial \tilde{F}}{\partial p}\right\}^T - \left[\frac{\partial \tilde{A}}{\partial p}\right][X] - [X]\left[\frac{\partial \tilde{A}}{\partial p}\right]^T \tag{73}$$

This is also a Lyapunov equation where the right-hand side is known. Following the derivations in Eq. (71),

$$\left[\frac{\partial \tilde{A}}{\partial p}\right] = [U]^{-1}\left[\frac{\partial V}{\partial p}\right] + [U]^{-1}\left[\frac{\partial U}{\partial p}\right][U]^{-1}[V] \tag{74}$$

Note that a number of matrices whose derivatives are required in the preceding equations depend on the set of modal vectors $[\phi]$ [Eqs. (3), (37), (41), and (46)]. Differentiation can be carried out assuming a fixed-mode[41] approach or a variable-mode approach. In the latter, variations of design variables lead to variations of the modal matrix used.

Application

The new methodology just derived has been implemented in an efficient, integrated aeroservoelastic design optimization capability, the Lifting Surface Augmented Structural Synthesis code (LS-CLASS)[6,7,37] and applied to a typical large, flexible commercial transport configuration. The structural model is based on an equivalent-plate formulation[32–36] for wing, control surfaces, and tail surfaces. Transverse shear effects are included. Horizontal- and vertical-plate segments are used for modeling of the complete configuration, with a fuselage modeled as a linked chain of beam/narrow-plate segments. The equivalent-plate approach, although not as general and accurate as the finite element (FE) method for the modeling of real airplanes, has nevertheless been found to be remarkably accurate—at least for research/conceptual design purposes—given its simplicity, ease of modeling, and special suitability for aeroelastic analysis. Its application to high-aspect-ratio and low-aspect-ratio wings has been studied thoroughly. With just a small number of degrees of freedom (of the order of 200–400), complete quite complex configurations can be modeled using equivalent plates, where FE models will require tens of thousands degrees of degrees of freedom. For the studies reported here, the doublet-lattice unsteady aerodynamics module of the Elfini[42] code was used to create full-order aerodynamic matrices for the Ritz functions used in LS-CLASS. These matrices were then imported into LS-CLASS and manipulated there. The equivalent plate model is shown in Fig. 2. The model consists of equivalent-plate segments (zones) joined via lumped springs, which model attachment and actuator stiffnesses. Spars, stringers, ribs, and skins are included in the model. The aerodynamic mesh is presented in Fig. 3. The wings, engines, horizontal stabilizers, and vertical fin are incorporated into the unsteady calculations. The fuselage aerodynamic distribution is introduced by scaling rigid airplane empirical distribution based on the local deformation along the fuselage centerline. There are no interference effects between the fuselage and the remaining aerodynamic surfaces. A block diagram of an active control system for symmetric motion (motion in the pitch plane) is shown in Fig. 4. The integrated aeroservoelastic model of the passenger jet configuration was checked against results obtained by standard industry codes, and the accuracy of the model used here was found to be good in terms of natural frequencies and mode shapes, deformation and local internal loads in maneuvers, as well as aeroservoelastic stability.

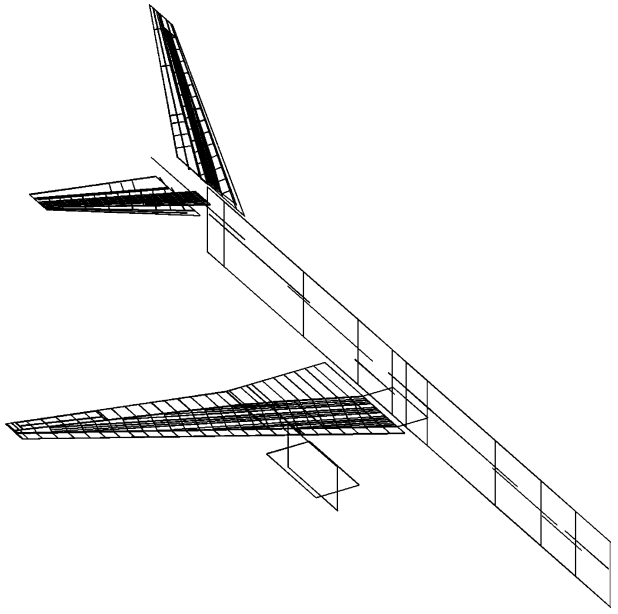

Fig. 2 Equivalent-plate structural model of a passenger airplane configuration.

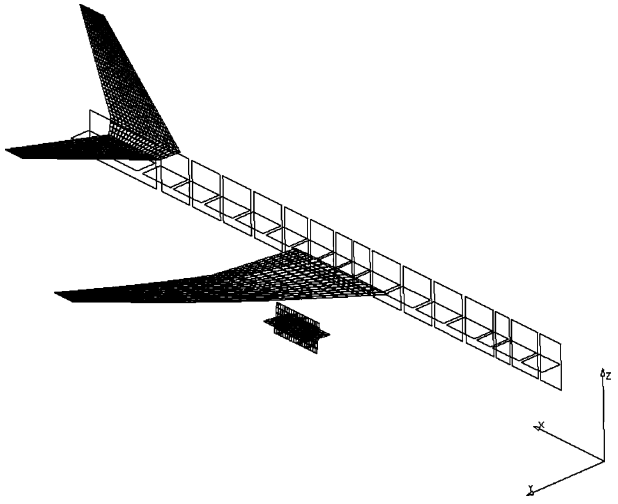

Fig. 3 Doublet-lattice aerodynamic mesh for the passenger airplane configuration.

Results of Convergence Studies

The stress covariance matrix and its sensitivity to a spar-cap-area design variable on the outboard wing have been calculated for a stress recovery point on the skin of the inboard wing. Figure 5 shows a comparison of the convergence characteristics between the MA method and the MD method for one of the covariance terms. These results are typical for all the matrix terms.

For the covariance matrix term the two methods will give the same results for a full-order model (165 modes; the model has 165 Ritz degrees of freedom, but a similarity transformation has been made to modal coordinates, i.e., no modal truncation). However, the MA method converges with 30–50 modes, whereas the MD needs at least 90 modes to converge. For the sensitivity term the MA method will converge with about 30–40 modes, whereas the MD will need about 120 modes for convergence.

The MA and MD methods do not converge to the same value for the sensitivity terms. This is actually an artifact of ignoring the eigenvector sensitivities in the analytical sensitivity calculations. Because for simplicity and better computational speed the MA sensitivity equations in the present formulation were based on a fixed-mode approach, finite differences had to be used to clarify this issue. A finite difference calculation of the sensitivities with a fixed modal base (FIXMOD) verifies that the two methods will yield different

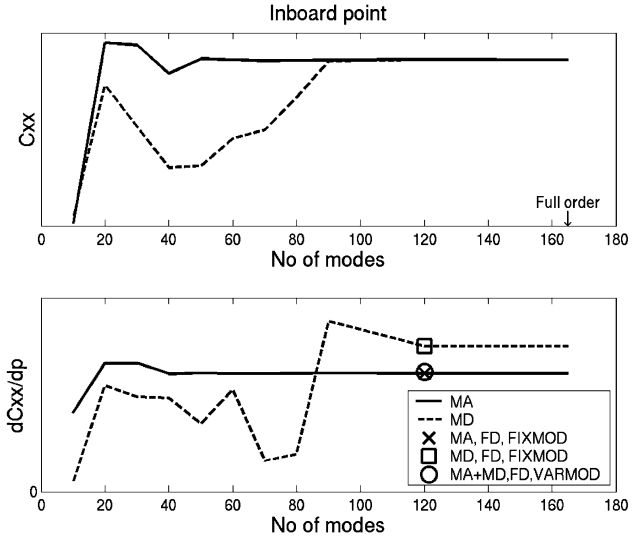

Fig. 5 Comparison of convergence of the MA method and the MD method for a stress covariance term and its sensitivity.

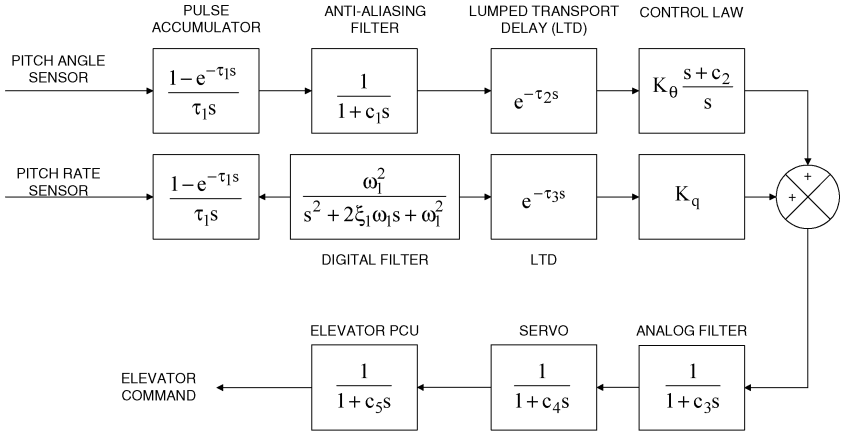

Fig. 4 Pitch control system definition.

results. Finite difference calculations with a variable (VARMOD) modal base will give the same results. It is also interesting that the finite difference calculations for the FIXMOD and VARMOD are practically identical for the MA method. The mode-acceleration results, then, converge to the correct value of sensitivity, and the effect of ignoring the eigenvector sensitivities in the MA analytical sensitivity calculations is basically negligible.

Taylor-Series Approximations

The key to the success of nonlinear programming in solving optimization problems is the use of approximation concepts. In each stage of the optimization process, a detailed analysis and the associated behavior sensitivity analysis are used for constructing approximations of the objective and constraint functions in terms of the design variables. The most common approximations are direct or reciprocal Taylor-series approximations.[31] These are local, linear approximations based on the Taylor series and vary with the design variable or the inverse of the design variable, respectively.

Taylor-series approximations are checked, using parametric studies, for a nominal flight case, with ample damping. Figure 6 shows the results when the design variable is a spar cap area of the outboard wing. Parametric studies for a closed-loop system, with a control gain as the design variable, are shown in Fig. 7. A direct linear Taylor-series approximation appears to capture accurately the variations of the stress covariance matrix terms with changes in the design variables in most cases. The fact that the linear approximation

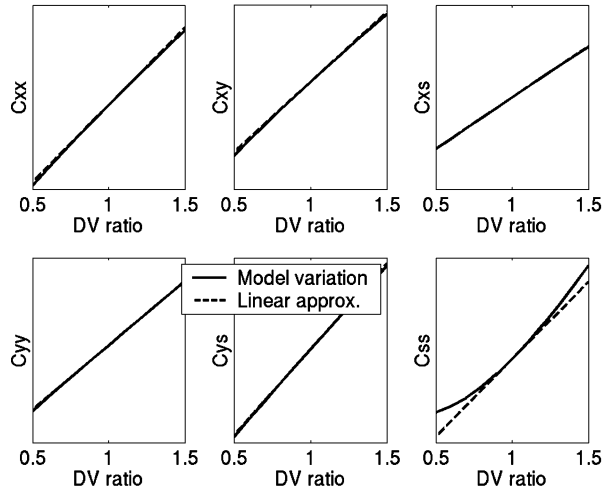

Fig. 6 Variation of covariance stresses with changes in a spar-cap-area design variable.

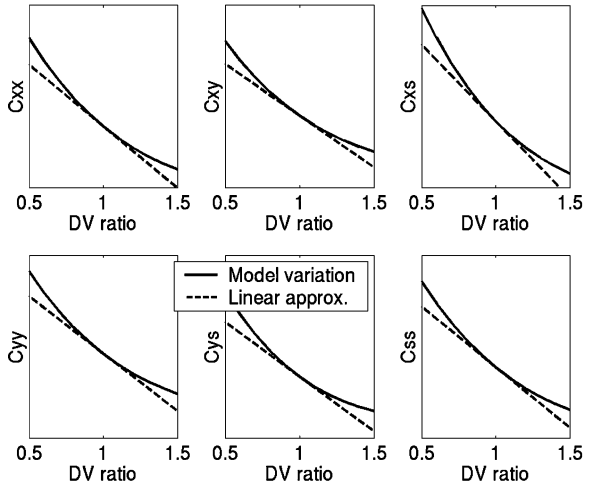

Fig. 7 Variation of covariance stresses with changes in a pitch control system gain design variable.

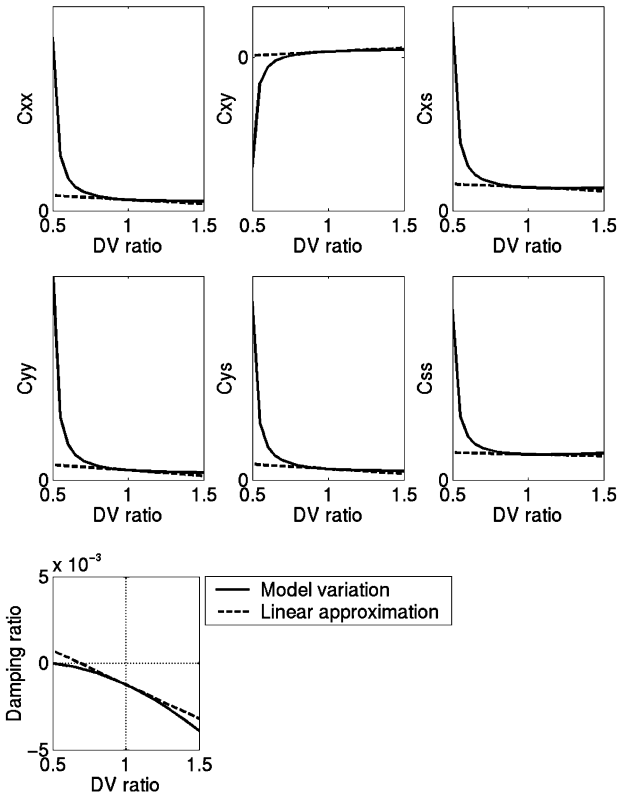

Fig. 8 Variation of covariance stresses with a spar-cap-area design variable (flight case with lightly damped mode approaching instability).

is tangent to the exact variation curve at the baseline configuration [design variable ratio = 1.0] indicates that the analytical sensitivity calculations are correct.

However, in airplane configurations with lightly damped structural modes, when in the course of design variable variation certain poles move toward instability, significant nonlinear behavior of the response might result. Figure 8 shows a flight case with a lightly damped mode close to instability. As the spar-cap-area design variable is reduced, the damping approaches zero. This results in a rise in the covariance matrix terms. It is apparent that a linear approximation cannot capture this explosive rise. A new approximation must be derived to capture these effects.

New Approximation

In the new approximation presented here, a Taylor-series approximation for the stress covariance matrix at a point (linear in the derivation included here) is augmented by a correction term as follows:

$$[\mathrm{Cov}_s] = [\mathrm{Cov}_s]_o + \sum_{k=1}^{N_k} \left(\left[\frac{\partial \mathrm{Cov}_s}{\partial p_k} \right]_o (p_k - p_{\mathrm{ko}}) + [\Delta \mathrm{Cov}_s(\{p\})] \right) \tag{75}$$

The summation is taken over N_k design variables, and the o denotes the reference configuration for which analysis and sensitivity analysis are carried out. The linear portion of the approximation can of course be replaced by a reciprocal approximation. To help guide the derivation of the correction term $[\Delta \mathrm{Cov}_s(\{p\})]$, we search for insight into the nature of the dependence of covariance terms on design variables. How does a pole approaching instability lead to explosive growth of the resulting response?

The stress covariance matrix [Eqs. (57) and (63–65)] can in general be calculated from the following diagonalization of the system matrix equations.[29] The MD state covariance matrix can be obtained from

$$[X] = [\Psi][Y][\Psi]^T \tag{76}$$

where the ij term of the matrix $[Y]$ is given by

$$Y_{ij} = \frac{(-[\Psi]^{-1}\{F\}Q\{F\}^T[\Psi]^{-T})_{ij}}{\lambda_i + \lambda_j} \tag{77}$$

The covariance matrix for stresses at a point is then

$$[\mathrm{Cov}_s] = [\eta]^T[A_L][X][A_L]^T[\eta] \tag{78}$$

The matrix of eigenvectors is $[\Psi] = [\psi_1 \ \ \psi_2 \ \ \cdots \ \ \psi_N]$, where the eigenvectors $\{\psi_i\}$ satisfy

$$[U]\{\psi_i\}\lambda_i = [V]\{\psi_i\} \tag{79}$$

Or, alternatively

$$\{\psi_i\}\lambda_i = [U]^{-1}[V]\{\psi_i\} = [\tilde{A}]\{\psi_i\} \tag{80}$$

If we define

$$[\Sigma]^T = [\Psi]^{-1} \tag{81}$$

where $[\Sigma] = [\xi_1 \ \ \xi_2 \ \ \cdots \ \ \xi_N]$, then,

$$Y_{ij} = \frac{-\{\xi_i\}^T\{F\}Q\{F\}^T\{\xi_j\}}{\lambda_i + \lambda_j} \tag{82}$$

Because of the presence of aeroservoelastic eigenvalues in the denominator, the covariance of the response shoots to infinity when the damping of any the aeroservoelastic modes approaches zero. This physical phenomenon is well known as flutter and is characterized by large response amplitudes often resulting in structural failure. It is assumed that the explosive behavior near instability is solely caused by the reduction of damping on some modes. The $[Y]$ matrix, then, depends on design variables through the dependence of aeroservoelastic eigenvalues λ_i on these design variables. Using a reference (baseline) design, the variation of $[Y]$ in the neighborhood of this design is described as the sum of a Taylor series in the design variables plus a correction term ΔY_{ij} to account for whatever the Taylor series cannot capture.

$$Y_{ij}(\{\boldsymbol{p}\}) = (Y_{ij})_o + \sum_k \left(\left(\frac{\partial Y_{ij}}{\partial \lambda_i}\right)_o \left(\frac{\partial \lambda_i}{\partial p_k}\right)_o + \left(\frac{\partial Y_{ij}}{\partial \lambda_j}\right)_o \left(\frac{\partial \lambda_j}{\partial p_k}\right)_o \right)(p_k - p_{k,o}) + \Delta Y_{ij}(\{\boldsymbol{p}\}) \tag{83}$$

In Eq. (83) $\{\boldsymbol{p}\}$ is the vector of design variables, and p_k is the kth design variable. The correction factor is, thus,

$$\Delta Y_{ij}(\{\boldsymbol{p}\}) = Y_{ij}(\{\boldsymbol{p}\}) - (Y_{ij})_o - \sum_k \left(\left(\frac{\partial Y_{ij}}{\partial \lambda_i}\right)_o \left(\frac{\partial \lambda_i}{\partial p_k}\right)_o + \left(\frac{\partial Y_{ij}}{\partial \lambda_j}\right)_o \left(\frac{\partial \lambda_j}{\partial p_k}\right)_o \right)(p_k - p_{k,o}) \tag{84}$$

The nominal $[Y]$ matrix at the reference (base) point is (using the values of aeroservoelastic poles and eigenvectors at the base point)

$$(Y_{ij})_o = \frac{-\{\xi_i\}_o^T\{F\}_o Q\{F\}_o^T\{\xi_j\}_o}{\lambda_{i,o} + \lambda_{j,o}} \tag{85}$$

The $[Y]$ matrix based on reference eigenvectors but changing eigenvalues (because of changes in the design variable vector $\{\boldsymbol{p}\}$) is given by

$$Y_{ij}(\{\boldsymbol{p}\}) = \frac{-\{\xi_i\}_o^T\{F\}_o Q\{F\}_o^T\{\xi_j\}_o}{\lambda_i(\{\boldsymbol{p}\}) + \lambda_j(\{\boldsymbol{p}\})} \tag{86}$$

Equation (85) and the numerator of Eq. (86) are evaluated at the base (reference) point once and are fixed for the approximations away from this base point. Only the eigenvalues are allowed to vary, and they are also evaluated using an approximation. In the case presented here, Rayleigh quotient approximations are used for the aeroservoelastic eigenvalues.

$$\lambda_i(\{\boldsymbol{p}\}) = \frac{\{\theta_i\}_o^T[V(\{p\})]\{\psi_i\}_o}{\{\theta_i\}_o^T[U(\{p\})]\{\psi_i\}_o} \tag{87}$$

where

$$[U(\{\boldsymbol{p}\})] = [U]_o + \sum_k \left[\frac{\partial U}{\partial p_k}\right]_o (p_k - p_{\mathrm{ko}})$$

$$[V(\{\boldsymbol{p}\})] = [V]_o + \sum_k \left[\frac{\partial V}{\partial p_k}\right]_o (p_k - p_{\mathrm{ko}}) \tag{88}$$

and $\{\theta\}$, $\{\psi\}$ are left and right eigenvectors, respectively, of the generalized eigenvalue problem [Eqs. (42) and (79)]. The correction term (beyond Taylor series) of the $[X]$ matrix is now

$$[\Delta X(\{\boldsymbol{p}\})] = \sum_i \sum_j \{\psi_i\}_o \Delta Y_{ij}(\{\boldsymbol{p}\})\{\psi_j\}_o^T \tag{89}$$

and, finally, the correction term for the stress covariance matrix is

$$[\Delta \mathrm{Cov}_s(\{\boldsymbol{p}\})] = [\eta]_o^T[A_L]_o[\Delta X(\{\boldsymbol{p}\})][A_L]_o^T[\eta]_o \tag{90}$$

The derivatives of terms of $[Y]$ with respect to the aeroservoelastic eigenvalues [Eqs. (84)] are obtained by differentiating Eq. (86), and evaluating the derivative at the reference point

$$\left(\frac{\partial Y_{ij}}{\partial \lambda_i}\right)_o = \left(\frac{\partial Y_{ij}}{\partial \lambda_j}\right)_o = \frac{\{\xi_i\}_o^T\{F\}_o Q\{F\}_o^T\{\xi_j\}_o}{(\lambda_{i,o} + \lambda_{j,o})^2} \tag{91}$$

Note that the correction term vanishes when the modal damping is large. The correction term has significant contribution only from lightly damped modes.

Approximate results (compared to "exact" parametric results) using the new stress covariance approximation are shown in Fig. 9. The method, indeed, captures the explosive rise in the covariance matrix terms, but because of inaccuracy of the eigenvalue approximation used this rise (based on the approximation) happens at a smaller design variable perturbation than in the exact case. It is not surprising, given the dependency of $[Y]$ on the eigenvalues λ, that the accuracy of the eigenvalue approximation used is extremely important.

In the approximate results presented so far, Rayleigh quotient eigenvalue approximations[43,44] were based on a fixed-mode approach. Changes in all eigenvectors were approximated. An improved approximation can be created if a mixed fixed/variable mode approach (where the right eigenvectors are allowed to vary but the left eigenvectors are kept fixed) is used for the Rayleigh quotient approximations (RQA).

$$\lambda_i(\{p\}) = \frac{\{\theta_i\}_o^T[V(\{\boldsymbol{p}\})]\{\psi_i(\{\boldsymbol{p}\})\}}{\{\theta_i\}_o^T[U(\{\boldsymbol{p}\})]\{\psi_i(\{\boldsymbol{p}\})\}} \tag{92}$$

where

$$\{\psi_i(\{\boldsymbol{p}\})\} = \{\psi_i\}_o + \sum_k \left\{\frac{\partial \psi_i}{\partial p_k}\right\}_o (p_k - p_{\mathrm{ko}}) \tag{93}$$

The eigenvector sensitivity can be calculated mode by mode[31,42] by a number of methods. Taking the derivative of Eq. (79) with respect to design value p_k results in

$$([U]\lambda_i - [V])\left\{\frac{\partial \psi_i}{\partial p}\right\} = \left(\left[\frac{\partial V}{\partial p_k}\right] - \lambda_i\left[\frac{\partial U}{\partial p_k}\right] - [U]\frac{\partial \lambda_i}{\partial p_k}\right)\{\psi_i\} \tag{94}$$

All terms here are evaluated at the reference configuration. The right-hand side of the equation is known. The matrix on the left side

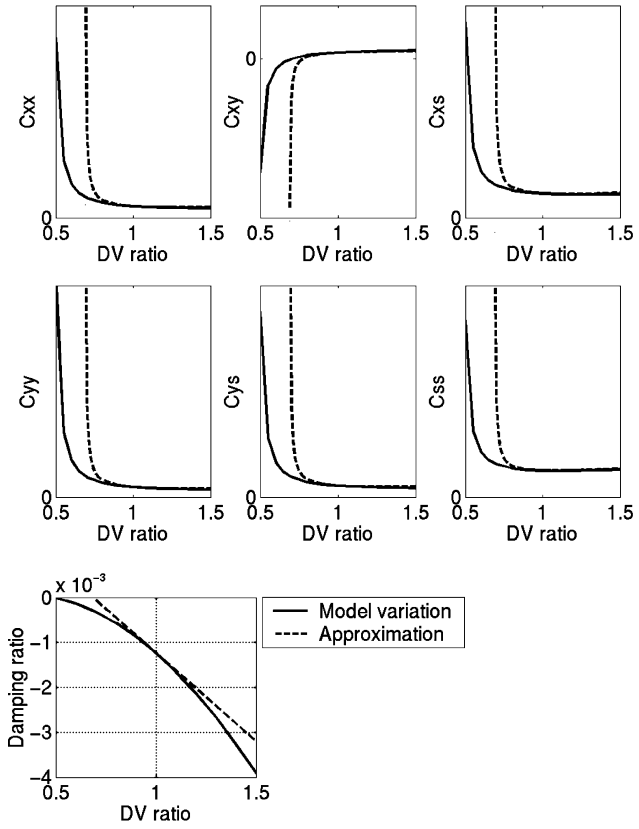

Fig. 9 New covariance approximation with standard RQA eigenvalue approximation for a spar-cap-area design variable (flight case with lightly damped mode approaching instability).

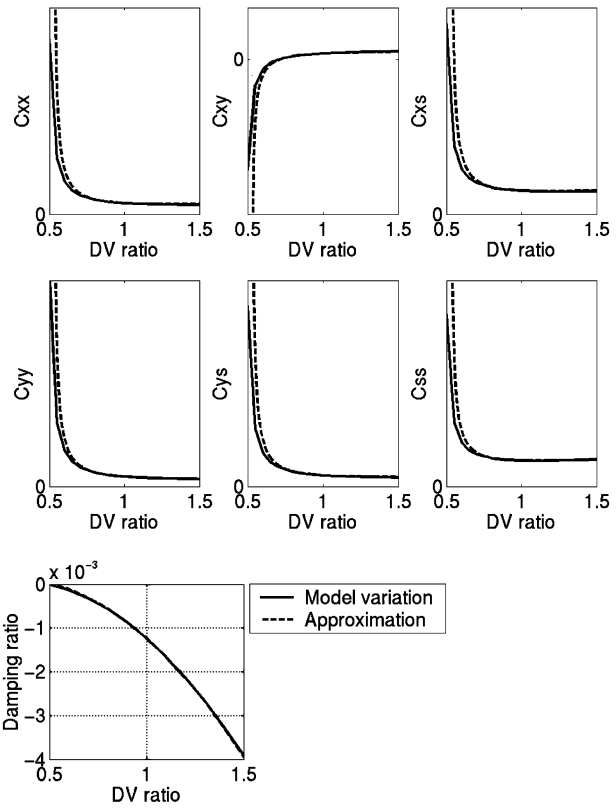

Fig. 10 New covariance approximation with new RQA eigenvalue approximation for spar-cap-area design variable (flight case with lightly damped mode approaching instability).

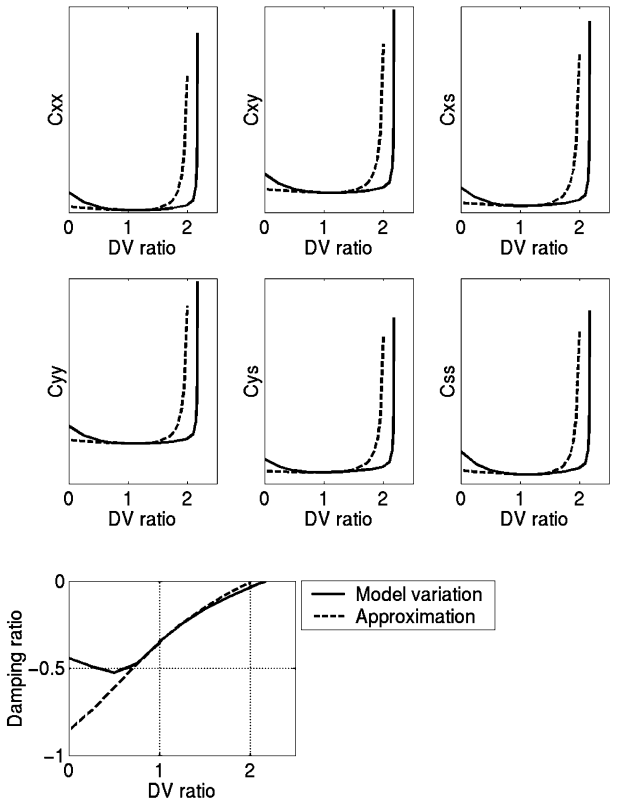

Fig. 11 New covariance approximation with standard RQA eigenvalue approximation for a control system gain design variable (flight case with a lightly damped mode approaching instability).

is singular, but the normalization criterion for the eigenvector can be used to eliminate this problem. When the eigenvector is normalized so that, for example, the mth term is constant, the mth term in the eigenvector sensitivity vector is zero. This criterion can be used to solve the equations to obtain the eigenvector sensitivity $\{\partial\psi_i/\partial p\}_o$ for Eq. (93).

Clearly, the calculation of eigenvector sensitivities of all modes with respect to all design variables adds considerable computational cost to the preparation of the approximations. However, because only very low damping in modes contributes significantly to the correction term just derived we can limit the number of eigenvalues for which a mixed fixed/variable mode RQA is calculated to only those with damping below some very low threshold value.

Figure 10 shows significant improvement in stress covariance response approximation when the improved eigenvalue approximations are used for the low damped modes. Figure 11 shows results from the new approximation for a flight case where an increase in control system gain makes the damping of the short period pitch mode unstable. The damping on the short period pitch mode is also shown in the figure. A mixed fixed/variable mode RQA is used for the short period mode in the new stress covariance approximation, and it is apparent that the new approximations capture the rise of the response well.

Results of additional studies and utilization of the new covariance matrix approximations for evaluating stress failure constraints for the integrated aeroservoelastic vehicle are described in Refs. 45 and 46.

Conclusions

A complete detailed formulation of the integrated aeroservoelastic gust stress response problem has been presented. The formulation is design oriented. That is, it introduces reduced-order modeling (in the form of a mode-acceleration method for random stresses), analytic sensitivities, and fast approximate analysis techniques. The new approximations are efficient and accurate. They are based on insight regarding the mathematical and physical nature of the effects

of design variable changes (structural or control) on the random stress response. Their importance is in the context of a nonlinear programming/approximation concepts multidisciplinary design optimization strategy.

The paper contains results of convergence studies to evaluate the new mode-acceleration adaptation. Convergence of both analysis and sensitivity solutions is examined. Performance of the new approximation is assessed using variation of both structural and control design variables. An integrated aeroservoelastic model of a passenger airplane configuration is used. The results presented here, then, apply to real configurations and realistic aerospace vehicle multi disciplinary optimization design challenges.

Appendix A: Case of Finite Element Structural Models

When detailed large-scale finite element models are used for the structural dynamic behavior of a flight vehicle, full-order aerodynamic matrices, corresponding to all degrees of freedom in the structural model, cannot be created using current lifting surface or panel methods. The aerodynamic matrices in the expression for full-order load vector, $[A^{ss}(s)][\phi]$, $[A^{sc}(s)]$, and $[A^{sg}(s)]$, are, in this case, obtained indirectly by what is known as the Summation of Forces and Moments method.[20,21] The number of rows in each of these matrices is the same as the number of degrees of freedom in the full-order finite element model, and they are obtained as follows.

On the aerodynamic mesh used to evaluate unsteady aerodynamic loads, the aerodynamic equation, for the case of lifting surface theory, for example, is

$$[AIC(M_\infty, s)]\{\Delta p\} = (q_D/U_\infty)\{w_n(s)\} \tag{A1}$$

where $[AIC]$is the aerodynamic influence coefficient matrix, Δp the pressure distribution, and w_n the normal velocity on the surface. Equation (A1) is solved for right-hand sides $\{w_n\}_j$ representing normal velocity distributions caused by a set of motion-shape generalized coordinates (vibration modes, Ritz vectors, polynomial functions, etc.). For general motions, which are expressed as superpositions of motions in the given generalized coordinates, the normalwash is given by

$$\{w_n\} = \sum \{w_n\}_j q_j \tag{A2}$$

The different pressure distributions $\{\Delta p\}_j$ can be integrated over the surface of the vehicle, and the resulting loads distributed to the nodes of the full-order structural mesh using a transformation

$$\{F_s\} = [T_1]\{\Delta p\} = \sum_j [T_1]\{\Delta p\}_j$$

$$= \frac{q_D}{U_\infty}[T_1][AIC]^{-1} \sum_j \{w_n\}_j q_j = [A^{ss}]\{q_s\} \tag{A3}$$

The matrices $[A^{sc}(s)]$ and $[A^{sg}(s)]$ are obtained in a similar form, representing forces on the full-order structural mesh caused by control-surface motions and gust excitations, respectively.

The rational function approximations (in the form of Roger or minimum-state approximants[38,39] can be used for the $[A^{ss}(s)][\phi]$, $[A^{sc}(s)]$, and $[A^{sg}(s)]$ mastrices obtained from Eq. (A3). To create the generalized aerodynamic matrices used for the mode-displacement equations (and their Roger or minimum-state approximation), the aerodynamic forces on the full-order structural mesh [obtained from Eq. (A3)] are integrated over the configuration to find the work they do when the configuration deforms in the motion-shape generalized coordinates one by one.

Appendix B: Viscous Damping Matrix

If the damping in the structure is assumed to be viscous, Ref. 17 shows that the nondiagonal damping matrix can be defined as

$$[C^{ss}] = [M^{ss}][\phi]([\phi]^T[M^{ss}][\phi])^{-1}$$

$$\times ([\phi]^T[C^{ss}][\phi])([\phi]^T[M^{ss}][\phi])^{-1}[\phi]^T[M^{ss}] \tag{B1}$$

The diagonal damping matrix can be defined as

$$[\phi]^T[C^{ss}][\phi] = [2\xi_i\omega_i]([\phi]^T[M^{ss}][\phi]) \tag{B2}$$

where $[2\xi_i\omega_i]$ is a diagonal matrix with $2\xi_i\omega_i$ along the diagonal. With this expression

$$[C^{ss}][\phi] = [M^{ss}][\phi]([\phi]^T[M^{ss}][\phi])^{-1}([\phi]^T[C^{ss}][\phi])$$

$$= [M^{ss}][\phi][2\xi_i\omega_i] \tag{B3}$$

See also Ref. 47.

The sensitivity of the damping matrix to a change in a design variable p is on the form

$$\left[\frac{\partial C^{ss}}{\partial p}\right][\phi] = \left[\frac{\partial M^{ss}}{\partial p}\right][\phi][2\xi_i\omega_i] + [M^{ss}][\phi]\left[2\xi_i \frac{\partial \omega_i}{\partial p}\right] \tag{B4}$$

Expression (B4) assumes that the sensitivities of the eigenvectors are zero. The eigenvectors and eigenvalues satisfy expression (B5).

$$[K^{ss}]\{\phi_i\} = [M^{ss}]\{\phi_i\}\omega_i^2 \tag{B5}$$

The sensitivity of expression (B5) with respect to design variables is shown in Eq. (B6), again with eigenvector sensitivities being zero.

$$\left[\frac{\partial K^{ss}}{\partial p}\right]\{\phi_i\} = \left[\frac{\partial M^{ss}}{\partial p}\right]\{\phi_i\}\omega_i^2 + [M^{ss}]\{\phi_i\}\frac{\partial \omega_i^2}{\partial p}$$

$$= \left[\frac{\partial M^{ss}}{\partial p}\right]\{\phi_i\}\omega_i^2 + [M^{ss}]\{\phi_i\}2\omega_i \frac{\partial \omega_i}{\partial p} \tag{B6}$$

By utilizing expression (B6), expression (B4) becomes

$$\left[\frac{\partial C^{ss}}{\partial p}\right][\phi] = \left[\frac{\partial M^{ss}}{\partial p}\right][\phi][\xi_i\omega_i] + \left[\frac{\partial K^{ss}}{\partial p}\right][\phi]\left[\frac{\xi_i}{\omega_i}\right] \tag{B7}$$

Here, $[\xi_i\omega_i]$ and $[\xi_i/\omega_i]$ are diagonal matrices with $\xi_i\omega_i$ and ξ_i/ω_i along on the diagonal, respectively.

References

[1]Hoblit, F. M., *Gust Loads on Aircraft: Concepts and Applications*, AIAA, Washington, DC, 1988, Chaps. 5 and 6.

[2]Houbolt, J. C., Steiner, R., and Pratt, K. G., "Dynamic Response of Airplanes to Atmospheric Turbulence Including Flight Data on Input and Response," NASA TR-R-199, June 1964.

[3]"Handbook for Aeroelastic Analysis," MSC/NASTRAN Ver. 65, MacNeal–Schwendler Corp., Los Angeles, CA, Nov. 1987.

[4]*Manual on Flight of Flexible Aircraft in Turbulence*, Advisory Group for Aerospace Research and Development, AGARD-AG-317, Neuilly sur Seine, France, May 1991.

[5]Livne, E., "Integrated Aeroservoelastic Optimization: Status and Direction," *Journal of Aircraft*, Vol. 36, No. 1, 1999, pp. 122–145.

[6]Livne, E., Schmit, L. A., and Friedmann, P. P., "Towards an Integrated Approach to the Optimum Design of Actively Controlled Composite Wings," *Journal of Aircraft*, Vol. 27, No. 12, 1990, pp. 979–992.

[7]Livne, E., Schmit, L. A., and Friedmann, P. P., "Integrated Structure/Control/Aerodynamic Synthesis of Actively Controlled Composite Wings," *Journal of Aircraft*, Vol. 30, No. 3, 1993, pp. 387–394.

[8]Bindolino, G., Ricci, S., and Mategazza, P., "Integrated Aeroservoelastic Optimization in the Design of Aerospace Systems," *Journal of Aircraft*, Vol. 36, No. 1, 1999, pp. 167–175.

[9]Karpel, M., "Reduced-Order Models for Integrated Aeroservoelastic Optimization," *Journal of Aircraft*, Vol. 36, No. 1, 1999, pp. 146–155.

[10]Karpel, M., Moulin, B., and Love, M. H., "Modal-Based Structural Optimization with Static Aeroelastic and Stress Constraints," *Journal of Aircraft*, Vol. 34, No. 3, 1997, pp. 433–440.

[11]Karpel, M., "Modal-Based Enhancement of Integrated Design Optimization Schemes," *Journal of Aircraft*, Vol. 35, No. 3, 1998, pp. 437–444.

[12]D'vari, R., and Baker, M., "Aeroelastic Loads and Sensitivity Analysis for Structural Loads Optimization," *Journal of Aircraft*, Vol. 36, No. 1, 1999, pp. 156–166.

[13]Zole, A., and Karpel, M., "Continuous Gust Response and Sensitivity Derivatives Using State-Space Models," *Journal of Aircraft*, Vol. 31, No. 5, 1994, pp. 1212–1214.

[14]Balis Crema, L., Mastrodi, F., and Coppotelli, G., "Aeroelastic Sensitivity Analyses for Flutter Speed and Gust Response," *Journal of Aircraft*, Vol. 37, No. 1, 2000, pp. 172–180.

[15]Bisplinghoff, R. L., and Ashley, H., *Principles of Aeroelasticity*, Dover, New York, 1975, pp. 350, 417.

[16]Hurty, W. C., and Rubinstein, M. F., *Dynamics of Structures*, Prentice–Hall, Upper Saddle River, NJ, 1964, pp. 299–307.

[17]Craig, R. R., *Structural Dynamics*, Wiley, New York, 1981, Chap. 15.

[18]Cornwell, R. E., Craig, R. R., Jr., and Johnson, C. P., "On the Application of the Mode-Acceleration Method to Structural Engineering Problems," *Earthquake Engineering and Structural Dynamics*, Vol. 11, No. 5, 1983, pp. 679–688.

[19]Blleloch, Paul, "Calculation of Structural Dynamic Forces and Stresses Using Mode Acceleration," *AIAA Journal*, Vol. 12, No. 5, 1988, pp. 760–762.

[20]Perry, B., III, Kroll, R. I., Miller, R. D., and Goetz, R. C., "DYLOFLEX: A Computer Program for Flexible Aircraft Flight Dynamic Loads Analysis with Active Controls," *Journal of Aircraft*, Vol. 17, No. 4, 1980, pp. 275–282.

[21]Pototzky, A. S., and Perry, B., "Dynamic Loads Analyses of Flexible Airplanes—New and Existing Techniques," AIAA Paper 85-0808, 1985.

[22]Arnold, R. R., Citerley, R. L., Chargin, M., and Galant, D., "Application of Ritz Vectors for Dynamic Analysis of Large Structures," *Computers and Structures*, Vol. 21, No. 5, 1985, pp. 901–908; also Vol. 21, No. 3, 1985, pp. 461–467.

[23]Kline, K. A., "Dynamic Analysis Using a Reduced Basis of Exact Modes and Ritz Vectors," *AIAA Journal*, Vol. 24, No. 12, 1986, pp. 2022–2029.

[24]Karpel, M., and Raveh, D., "The Fictitious Mass Element in Structural Dynamics," *AIAA Journal*, Vol. 34, No. 3, 1996, pp. 607–613.

[25]Livne, E., and Blando, G. D., "Reduced Order Design-Oriented Stress Analysis Using Combined Direct and Adjoint Solutions," *AIAA Journal*, Vol. 38, No. 5, 2000, pp. 898–909.

[26]Livne, E., and Blando, G. D., "Structural Dynamic Frequency Response Using Combined Direct and Adjoint Reduced-Order Approximations," *AIAA Journal*, Vol. 41, No. 7, 2003, pp. 1377–1385.

[27]Bryson, A. E., and Ho, Y-C., *Applied Optimal Control*, Ginn and Co., Waltham, MA, 1969, Chap. 10 and 11.

[28]Mukhopadhyay, V., Newsome, J. R., and Abel, I., "A Method for Obtaining Reduced-Order Control Laws for High Order Systems Using Optimization Techniques," NASA TP-1876, Aug. 1981.

[29]Livne, E., "Alternative Approximations for Integrated Control/Structure Aeroservoelastic Synthesis," *AIAA Journal*, Vol. 31, No. 6, 1993, pp. 1100–1108.

[30]Schmit, L. A., "Structural Optimization—Some Key Ideas and Insights," *New Directions in Optimum Structural Design*, edited by E. Atrek, R. H. Gallagher, K. M. Ragsdell, and O. C. Zienkiewicz, Wiley, New York, 1984.

[31]Haftka, R. T., and Gurdal, Z., *Elements of Structural Optimization*, 3rd ed., Kluwer Academic, Norwell, MA, 1992, Chap. 6.

[32]Giles, G. L., "Equivalent Plate Modeling for Conceptual Design of Aircraft Wing Structures," AIAA Paper 95-3945, Sept. 1995.

[33]Giles, G. L., "Design Oriented Analysis of Fuselage Structures Using Equivalent Plate Methodology," *Journal of Aircraft*, Vol. 36, No. 1, 1999, pp. 21–28.

[34]Livne, E., Sels, R. A., and Bhatia, K. G., "Lessons from Application of Equivalent Plate Structural Modeling to an HSCT Wing," *Journal of Aircraft*, Vol. 31, No. 4, 1994, pp. 953–960.

[35]Stone, S. C., Henderson, J. L., Nazari, M. M., Boyd, W. N., Becker, B. T., Bhatia, K. G., Giles, G. L., and Wrenn, G. A., "Evaluation of Equivalent Laminated Plate Solution (ELAPS) in HSCT Sizing," AIAA Paper 2000-1452, April 2000.

[36]Livne, E., "Equivalent Plate Structural Modeling for Wing Shape Optimization Including Transverse Shear," *AIAA Journal*, Vol. 32, No. 6, 1994, pp. 1278–1288.

[37]Livne, E., "Integrated Multidisciplinary Optimization of Actively Controlled Fiber Composite Wings," Ph.D. Dissertation, Dept. of Mechanical, Aerospace, and Nuclear Engineering, Univ. of California, Los Angeles, Sept. 1990.

[38]Roger, K. L., "Airplane Math Modeling Methods for Active Control Design," *Proceedings of the 44th AGARD Structures and Material Panel*, Structural Aspects of Active Controls, AGARD-CP-228, Lissabon, Portugal, April 1977, pp. 4.1–4.11.

[39]Karpel, M., "Time Domain Aeroservoelastic Modeling Using Weighted Unsteady Aerodynamic Forces," *Journal of Guidance, Control, and Dynamics*, Vol. 13, No. 1, 1990, pp. 30–37.

[40]Campbell, C. W., "Monte Carlo Turbulence Simulation Using Rational Approximations to Von Karman Spectra," *AIAA Journal*, Vol. 24, No. 1, 1986, pp. 62–66.

[41]Haftka, R. T., and Yates, E. C., "Repetitive Flutter Calculations in Structural Design," *Journal of Aircraft*, Vol. 13, No. 7, 1976, pp. 454–461.

[42]Nicot, P., and Petiau, C., "Aeroelastic Analysis Using Finite Element Models," DGLR/AAAF/RAES, European Forum on Aeroelasticity and Structural Dynamics, Aachen, Germany, April 1989.

[43]Canfield, R. A., "High Quality Approximation of Eigenvalues in Structural Optimization," *AIAA Journal*, Vol. 28, No. 6, 1990, pp. 1116–1122.

[44]Canfield, R. A., "Design of Frames Against Buckling Using a Rayleigh Quotient Approximation," *AIAA Journal*, Vol. 31, No. 6, 1993, pp. 1143–1149.

[45]Engelsen, F., and Livne, E., "Design-Oriented Quadratic Stress Failure Constraints for Actively Controlled Structures under Combined Steady and Random Excitation," *AIAA Journal* (to be published).

[46]Engelsen, F., "Design-Oriented Gust Stress Constraints for Aeroservoelastic Design Synthesis," Ph.D. Dissertation, Dept. of Aeronautics and Astronautics, Univ. of Washington, Seattle, Aug. 2001.

[47]Karpel, M., and Wieseman, C. D., "Modal Coordinates for Aeroelastic Analysis with Large Local Structural Variations," *Journal of Aircraft*, Vol. 31, No. 2, 1994, pp. 396–403.